

Synthesis and Characterization of a Temperature-Sensitive Microcapsule Gelling Agent for High-Temperature Acid Release

Yunfeng Liu,* Lang Zhou, Xiaochun Wan, Yongfan Tang, Qiang Liu, Wei Li, and Jianbo Liao

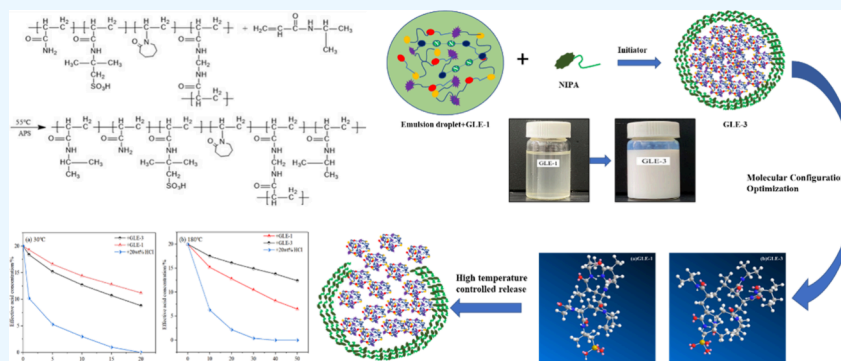
Cite This: *ACS Omega* 2024, 9, 20849–20858

Read Online

ACCESS |

Metrics & More

Article Recommendations



ABSTRACT: Deep, high-temperature carbonate reservoirs, represented by the Chuanzhong-Gaomo Block and the Penglai Gas Field, have become important supports for increased storage and production in Sichuan Basin. However, acidization in high-temperature to ultrahigh-temperature reservoirs faces several technical challenges, such as fast acid-rock reaction rates, limited acid corrosion distances, and high risks of tubular corrosion. In this study, a novel high-temperature-resistant microencapsulated gelling agent GLE-3 was prepared using *N*-isopropylacrylamide (NIPAM) as the wall material, acrylamide (AM), 2-acrylamido-2-methylpropanesulfonic acid (AMPS), and *N*-vinylcaprolactam (NVCL) as the core materials, and *N,N'*-methylenebis(acrylamide) (MBA) as the cross-linking agent through inverse emulsion polymerization. GLE-3 was structurally characterized using infrared spectroscopy, transmission electron microscopy, and particle size analysis, and its properties were evaluated. The results showed that GLE-3 exhibited uniform particle size distribution ranging from 10 to 100 μm . Under high-temperature conditions of 180 $^{\circ}\text{C}$ and a shear rate of 170 s^{-1} , the viscosity of the gel acid solution remained above 27.8 $\text{mPa}\cdot\text{s}$, with a viscosity retention rate of 63.76%. Compared to GLE-1 (uncapsulated), GLE-3 demonstrated improved thermal stability and shear stability after microencapsulation. After 60 min of shearing at 180 $^{\circ}\text{C}$ and shear rate of 170 s^{-1} , the viscosity retention rate was 88.99%. Furthermore, under 180 $^{\circ}\text{C}$ conditions, GLE-3 exhibited good high-temperature slow-release performance compared to GLE-1, which uncapsulated with the same raw materials. By increasing the viscosity of the gel acid, delaying the acid-rock reaction rate, and providing high-temperature slow-release effects, the high-temperature resistance of the acid system was enhanced, ultimately achieving deep acidization in high-temperature reservoirs.

1. INTRODUCTION

As deep and ultradeep marine carbonate reservoirs continue to be developed, the high-temperature conditions in the strata pose elevated technical requirements for the acidizing fluids used in reservoir modification. For instance, in the Penglai gas field of the central Sichuan uplift, reservoir temperatures can exceed 180 $^{\circ}\text{C}$, rendering conventional acidizing fluid technologies inadequate to meet on-site demands.^{1–3} The primary challenges encountered during high-temperature reservoir acidization processes include:^{4–6} (1) as reservoir temperature increases, the reaction rate of acid with rock accelerates, resulting in a shorter effective acid penetration distance and difficulties in achieving deep penetration; (2) at higher reservoir temperatures, the corrosive effects of acid

become more pronounced, leading to increased corrosion and damage to the wellbore casing. Therefore, effectively controlling the acid-rock reaction rate and enhancing acid etching distance to achieve deep penetration in the process of high-temperature carbonate reservoir acidization are crucial prerequisites for efficient carbonate reservoir modification. Gel

Received: December 1, 2023

Revised: March 21, 2024

Accepted: March 22, 2024

Published: April 30, 2024



acid is a viscous acid fluid system primarily composed of gelling agents, coupled with corrosion inhibitors, iron ion stabilizers, clay stabilizers, and other components. By introducing suitable gelling agents into the acid fluid, the overall viscosity of the acid is increased, thereby retarding the migration speed of hydrogen ions toward the rock surface. This, in turn, slows down the acid-rock reaction rate and effectively extends the acid etching distance. Currently, gel acid systems have been widely applied in the modification of carbonate reservoirs both domestically and internationally, demonstrating favorable reservoir modification results and economic benefits. However, with the ongoing development of deep and ultradeep carbonate oil and gas reservoirs, there is an increasing number of wells with temperatures exceeding 180 °C, demanding higher technical performance for acid fluid resistance to high temperatures. Particularly, as the temperature rises to a certain degree, under continuous pumping of acid fluid in dynamic conditions, the ultrahigh temperature and shear conditions significantly affect the viscosity of the acid fluid. After a period of shearing, the viscosity of the acid fluid sharply drops, ultimately losing its ability to delay the acid-rock reaction rate and failing to achieve the objective of deep penetration.^{3,7} The main reason for this lies in the fact that under ultrahigh temperature and shear conditions, the rigidity and ion groups of existing cationic polymer gelling agents are prone to fracture and failure in highly concentrated acid fluids. Therefore, addressing the challenge of gelling agents for ultrahigh-temperature acid fluids effectively requires a key focus on balancing acid solubility and high-temperature resistance, either through the design of polymer molecular structures or from a new conceptual perspective.

In recent years, scholars both domestically and internationally have undertaken numerous endeavors in the development of novel polymer materials for ultrahigh-temperature applications. The key information is available in Table 1.

It is evident that research on polymer-based gelling agents for environments characterized by ultrahigh temperatures and high acid concentrations faces challenges, as individual polymers typically exhibit temperature resistance not exceeding 180 °C. Moreover, most studies are currently in the laboratory experimentation phase, thereby falling short of meeting on-site application demands.^{14–16} Since the 1980s, the membrane stress rupture mechanism and membrane permeation release mechanism have considered the permeation release mechanism to be reliable. Under high-temperature conditions, permeation release is predominant, while under high pressure, membrane stress rupture release takes precedence. Drawing upon the concept of microcapsule-controlled release, scholars have introduced microencapsulation technology into the field of acid fluid material development, undertaking exploratory research efforts. Li et al.¹⁷ addressed the challenge of plugging difficulties during drilling and employed paraffin as the wall material to prepare microcapsules of highly water-absorbent resin using a melt dispersion condensation method. Simultaneously, ABS resin was used to encapsulate the initiator 2,2'-azodi (2-methylpropionamide) dihydrochloride to prolong the gelation time of polyacrylamide cross-linked gel. The results demonstrated an extension of gelation time by more than eight times, effectively addressing issues related to short gelation time and poor plugging efficiency. Song et al.¹⁸ utilized cyclodextrin to prepare azalea microcapsules, evaluating parameters such as encapsulation rate, efficacy, and saturation temperature. The study verified the positive impact of

Table 1. Gelling Agents Developed by Different Scholars

authors	main raw materials	main performance
Wang et al. ⁸	AMPS/AM/H-DMDAAC (diallyldimethylammonium chloride)	high-viscosity retention at elevated temperatures and is suitable for hydraulic fracturing operations at 180 °C and above
Li et al. ⁹	AM/AMPS/DMDAAC/DMC (methacryloxyethyltrimethyl ammonium chloride)	superior thickening, temperature resistance, and shear resistance properties, withstanding temperatures up to 160 °C
Sui et al. ¹⁰	modified xanthan gum	excellent temperature resistance, acid resistance, and shear resistance, maintaining a viscosity of 21 mPa·s at 160 °C
Wang et al. ¹¹	AM/DAC	have a resistance reduction rate of 68.5% at 180 °C, the apparent viscosity remains at 23 mPa·s after shearing at a rate of 170 s ⁻¹ for 70 min
Sun et al. ¹²	AM/AMPS/hydrophobic monomers/vinyl polysilsesquioxane nanoparticles	characterized by low dosage, easy solubility in acid, and excellent retardation performance, exhibits prominent thickening effects; at a shear rate of 170 s ⁻¹ , when 2.0 wt % of the gelling agent is dissolved in 20 wt % hydrochloric acid at room temperature, the apparent viscosity of the acid fluid reaches 51 mPa·s; even at 180 °C, the apparent viscosity of the gel acid fluid remains above 15 mPa·s
Mohammed et al. ¹³	single-phase acid system composed of alkyl sulfonic acid	under conditions of 20.68 MPa and 82–177 °C, the diffusion coefficient of the acid fluid is comparable to that of a 15 wt % HCl emulsified acid system

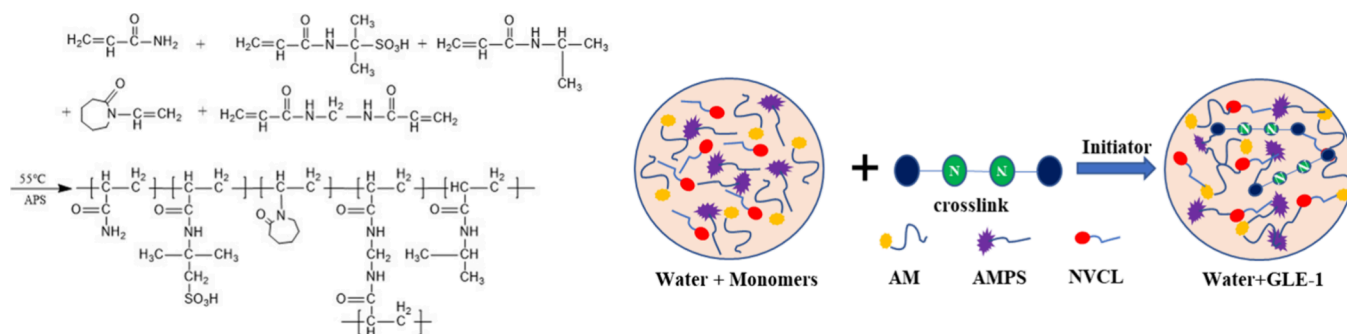


Figure 1. Preparation process and molecular structure formula of GLE-1.

microcapsules on the acid's effectiveness. Singh et al.¹⁹ encapsulated 10% hydrochloric acid with highly hydrophobic silica nanoparticles, forming microcapsules. This not only reduced the experimental time of the acid fluid but also enhanced its thermal stability. The microcapsules exhibited temperature resistance up to 80 °C and compared to the oil-encapsulated acid emulsion, the acid release time was more than doubled. Postacid release and etching occurred on the fracture surface, and microencapsulated acid fluid enhanced the fracture conductivity of shale formations. Zhang et al.²⁰ aimed to mitigate the damage caused to reservoirs during the fracturing process, such as invasion of fracturing fluid filtration and solid residue after gel breakage. They developed a fracturing-blocking protective agent, TD-1, using organic acid as the core material, ethyl cellulose as the capsule material, polyvinylpyrrolidone as the porosity inducer, and poly(vinyl alcohol) as the protective agent. The prepared TD-1 had a particle size of approximately 300 μm , an organic acid content of 34.1%, and a release rate of 69.0%. It could form a temporary blocking zone on the reservoir surface, reducing damage caused by fracturing fluid filtration and solid-phase substance invasion. Ji et al.²¹ highlighted the significant loss of viscosity experienced by polymer solutions subjected to strong shear during the application of dry powder polymer flooding materials. Utilizing polyurea microcapsules as shell materials to encapsulate emulsion polymer particles, they prepared spherical microcapsule emulsion polymers with a particle size distribution of 100–600 nm, exhibiting excellent sustained release and thickening capabilities. Essifi et al.²² developed various organic and hybrid systems for quercetin encapsulation, including Ca-Alginate (Qr-Alg), Ca-Alginate@Na-montmorillonite (Qr-Alg@Na-Mnt), and Ca-Alginate@CPC-montmorillonite (Qr-Alg@CPC-Mnt). Subsequently, they investigated the release kinetics principles of quercetin molecules in two different aqueous media within organic microcapsules and hybrid microcapsules. According to the above analysis, microcapsules can better improve the temperature resistance and slow release performance of the gelling agent. In this study, monomer with good temperature resistance and acid resistance is selected. For example, AM, AMPS, and NVCL are preferred. NIPAM is temperature sensitive and can be released when a certain temperature is reached, so it is used as a wall material for gelling agents.

It is evident that under high-temperature to ultrahigh-temperature conditions, the standalone use of existing polymer-based gelling agents is ineffective in effectively delaying the acid-rock reaction rate. Microencapsulation technology, with its delayed release characteristics, offers a potential solution. This approach involves encapsulating

polymer gelling agents within microcapsules, wherein the capsule wall material ruptures under specific temperature or pressure conditions, releasing the core material (the polymer). This release triggers the maintenance of acid fluid viscosity under high-temperature conditions, thereby achieving effective control over the viscosity of the gelling acid fluid. Ultimately, this approach facilitates the desired goal of deep penetration for reservoir modification.

2. MATERIALS AND METHODS

2.1. Materials. In the experiments, the following chemical materials were primarily utilized: anhydrous ethanol, deionized water, acrylamide, *N*-isopropylacrylamide, *N*-vinylcaprolactam, anhydrous sodium sulfite, ammonium persulfate, 2-acrylamido-2-methylpropanesulfonic acid, and *N,N'*-methylenebis(acrylamide), all procured from China National Pharmaceutical Group Corporation. High-purity nitrogen gas was obtained from Tianyuan Gas Manufacturing Co., Ltd.

The instruments employed in the experiments included a Brookfield DV2T rotational viscometer, procured from Brookfield Corporation, USA, a GLS-4 digital high-speed stirrer from Shandong Meiling Scientific Instruments Co., Ltd., a constant temperature water bath from Changzhou Yawang Instruments Co., Ltd., and a blast drying oven from Shanghai Yitian Science Instrument Co., Ltd. Three-necked flasks, beakers, measuring cylinders, and glass stoppers were purchased from glassware manufacturers. An electronic analytical balance (JC-TP model) was acquired from Jingcheng Instruments Co., Ltd. A laser particle size analyzer was obtained from Liaoning Dandong Baiter Corporation. The Nexus Fourier transform infrared spectroscopy analyzer was purchased from Nicolet Corporation, USA.

2.2. Methods. **2.2.1. Preparation of Comparative Samples for Gelling Agents.** The preparation of the comparative gel samples GLE-1 was conducted using a water-soluble polymerization method, following the procedure outlined below: 20.0 g of monomer was dissolved in 40.0 g of water in which the mass ratio of acrylamide, 2-acrylamide-2-methylpropanesulfonic acid, *n*-vinylcaprolactam, and *n*-isopropylacrylamide is 6:3:1:10, and 0.002 g of cross-linker and 0.05 g of initiator were added (the mass ratio of ammonium persulfate to anhydrous sodium sulfite is 6:4). Under nitrogen protection, the reaction was carried out at a temperature of 35 °C for 4 h. The resulting product was repeatedly washed with ethanol and subjected to freeze-drying.²³ The gel agent GLE-1 was obtained, and the preparation principle and molecular structure are illustrated in Figure 1.

2.2.2. Preparation of Microcapsule Gel. The preparation of microcapsule coagulant was conducted using a reverse

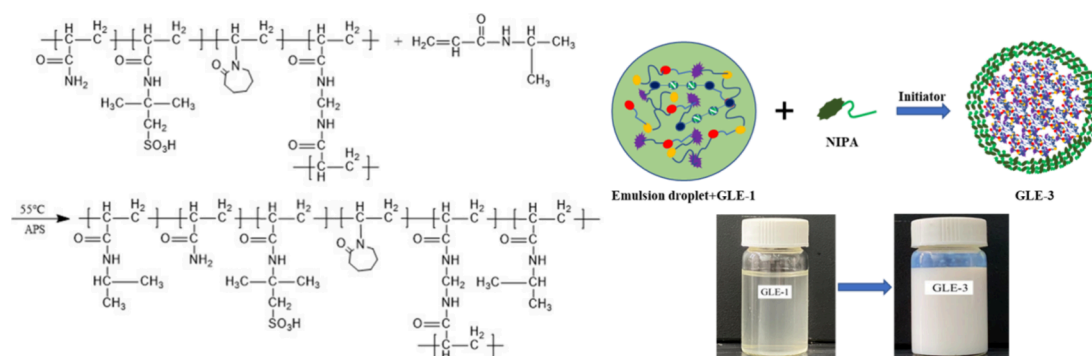


Figure 2. Preparation process and molecular structure formula of GLE-3.

emulsion polymerization method in which kerosene was selected as the continuous phase and water as the dispersed phase. The specific preparation steps are as follows:^{24,25} (1) for preparation of the continuous phase: 0.3 g of sodium dodecyl sulfonate was dissolved in 20.0 g of kerosene and stirred for a certain amount of time to ensure complete dissolution. (2) For preparation of the dispersed phase: 6.0 g of acrylamide, 3.0 g of 2-acrylamide-2-methylpropanesulfonic acid, and 1 g of *N*-vinylcaprolactam were dissolved in 30.0 g of water, and 0.02 g of ammonium persulfate and 0.015 g of sodium sulfite anhydrous were added and reacted at 35 °C for 2 h. *N*-Isopropylacrylamide (10.0 g) was added to the completed reaction mixture, and stirring was performed to ensure dissolution. Subsequently, after adding 0.01 g of ammonium persulfate and 0.005 g of anhydrous sodium sulfite, 0.002 g of cross-linking agent *N,N'*-methylenebis(acrylamide) was slowly added. (3) The dispersed phase was slowly added dropwise to the continuous phase, and emulsification was carried out using an emulsifying shear mixer. (4) Under nitrogen protection, the reaction was carried out for 2 h at a specified temperature. The resulting product was subjected to centrifugation separation under nitrogen protection, followed by repeated washing with ethanol. The product was then placed in a freeze-dryer for freeze-drying. The microcapsule coagulant product, denoted as GLE-3, was obtained. The preparation process and molecular structure diagram are shown in Figure 2.

2.2.3. Performance Evaluation of Microcapsule Coagulants.

1. For preparation of coagulation acid, 20 wt % hydrochloric acid solution was chosen as the base liquid to which varying amounts of coagulant and high-temperature corrosion inhibitors were separately added, forming experimental acid solutions.
2. For particle size distribution testing of microcapsule coagulant, a certain quantity of microcapsule coagulant (GLE-3) was taken, and its particle size distribution was analyzed using the Bettersize 3000Plus fully automatic laser particle analyzer.
3. For infrared spectroscopy of microcapsule coagulant, the American Thermo Fisher Nicolet ISS FT-IR spectrometer was employed to examine the characteristic peaks of major functional groups in the microcapsule coagulant GLE-3. This analysis aimed to assess whether the molecular structure of the product met the design specifications.
4. For thermal stability experiment, with a preferred coagulant concentration of 1.0 wt %, a HAAKE Viscotester iQ rheometer was utilized to measure the

peak apparent viscosity of the acid solution at temperatures of 30 (room temperature), 60, 90, 120, 150, and 180 °C. Simultaneously, the viscosity retention percentage of the acid solution under different temperature conditions was calculated based on the difference between the peak apparent viscosity after the high-temperature shear and the peak apparent viscosity at room temperature.

5. For thermal dilution experiment, the optimal addition of acid solution coagulant was set at 1.0 wt %. Different coagulation acids were placed in a constant temperature water bath at 30, 40, 50, 60, 70, 80, and 90 °C for 60 min. The variations in the apparent viscosity of the coagulation acid with temperature were then examined.
6. For temperature and shear stability experiment, with a preferred coagulant concentration of 1.0 wt %, a HAAKE Viscotester iQ rheometer was employed to measure the dynamic shear conditions at 170 s⁻¹, gradually heating to 180 °C. The changes in the apparent viscosity of different coagulation acids with shear time were then assessed. Additionally, the percentage of retention of peak apparent viscosity after high-temperature shear for 60 min was calculated.
7. For retardation performance experiment, in accordance with SY/T5886-2018 “Method for evaluating the performance of acidizing working fluids” and SY/T6214-2016 “Thickener for Thickening Acid”,^{8,26} GLE-1 acid, GLE-3 acid, and 20 wt % hydrochloric acid formulation were selected. Using a sodium hydroxide solution, the acid–base titration method was employed at temperatures of 30 and 180 °C to test the effective acid concentration of the remaining acid after different reaction times. Comparative analysis was conducted to evaluate the retardation performance of different acid solutions.

3. RESULTS AND ANALYSIS

3.1. Performance Characterization. 3.1.1. Particle Size Distribution of Microcapsule Coagulants.

The particle size of the prepared microcapsule coagulant was analyzed using the Bettersize 3000 laser particle size analyzer. Prior to testing, the microcapsule coagulant was introduced into water to create a homogeneous suspension. The experimental results are depicted in Figure 3.

The data from Figure 3 reveals that the prepared microcapsule coagulant exhibits a relatively uniform particle size distribution with a narrow range, predominantly distributed within the range of 10–100 μm. The average

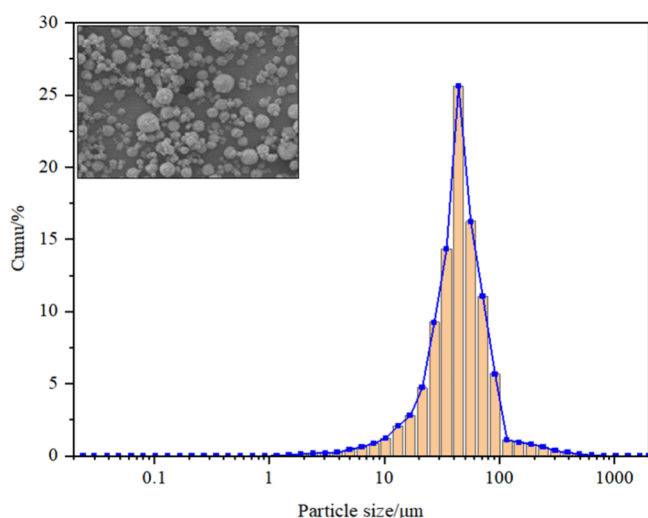


Figure 3. Particle size distribution curve of GLE-3.

particle size is measured at $53.22 \mu\text{m}$, indicative of a diminutive particle size. Furthermore, the particle size distribution exhibits a narrow span, suggesting a high degree of uniformity. This diminution in particle size and concomitant narrow distribution range minimizes the likelihood of blockages occurring during the transportation process down the wellbore.²⁷

3.1.2. Infrared Spectroscopy of Microcapsule Coagulants. After cleaning and purifying the prepared microcapsule gel sample, it was pressed into tablets and a Fourier transform infrared spectrometer was used to test its infrared spectrum. The results are shown in Figure 4.

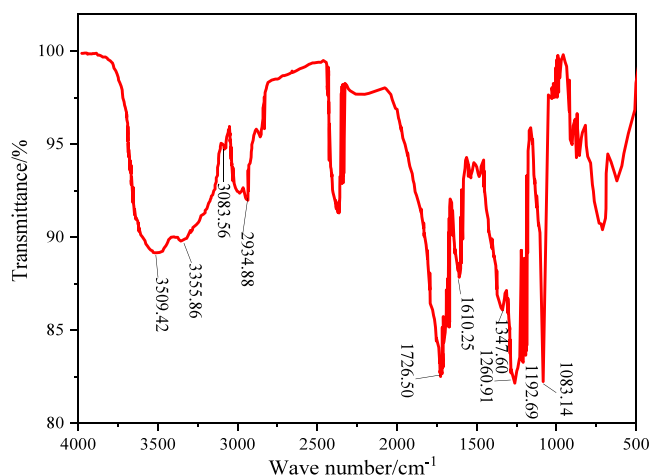


Figure 4. Infrared spectral curve of GLE-3.

The infrared spectroscopy curve indicates distinctive absorption peaks associated with functional groups. Peaks at wavenumbers 3509.42 and 3355.86 cm^{-1} correspond to characteristic hydroxyl group absorptions. Peaks at wavenumbers 3083.56 and 1610.25 cm^{-1} are indicative of amide group absorptions, while the peak at 1347.60 cm^{-1} corresponds to the characteristic absorption of isopropyl groups. The presence of a peak at 2934.88 cm^{-1} is associated with methyl groups. Additionally, peaks at wavenumbers 1192.69 and 1083.14 cm^{-1} represent characteristic absorptions of sulfonic acid groups. These spectral features collectively affirm the successful synthesis of the designed product.

3.1.3. Thermal Stability Evaluation. Thermal stability is one of the fundamental parameters for characterizing the temperature resistance of acid solutions. During the experiment, the apparent viscosity of the gelled acid after high-temperature treatment was tested at room temperature, and the viscosity retention rate of the acid solution before and after high-temperature reaction was calculated. The experimental data from Figure 5 illustrates that the coagulating acid

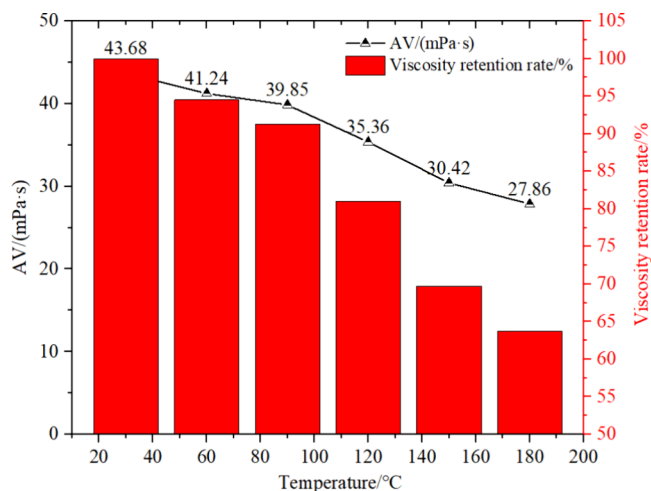


Figure 5. Thermal stability of GLE-3 gelling agent under different temperature conditions.

formulated with coagulant GLE-3 maintains a viscosity retention exceeding 80% after heating for 4 h in the temperature range of $30\text{--}120 \text{ }^{\circ}\text{C}$, followed by cooling to $30 \text{ }^{\circ}\text{C}$. Experimental observations reveal the absence of conspicuous precipitation and a negligible increase in turbidity in the coagulating acid after heating, indicating the excellent thermal stability of the coagulating acid prepared with GLE-3. Moreover, even after heating for 4 h at 150 and $180 \text{ }^{\circ}\text{C}$, the viscosity retention remains above 63%, underscoring the commendable thermal stability of the coagulant. The elevated viscosity retention postheating and subsequent decrease in temperature suggest that the high temperature induces molecular chain extension, and upon temperature reduction, the molecular structure of the coagulant regains its original form, leading to an increase in the viscosity of the coagulating acid system.²⁸ Considering the microcapsule structure of GLE-3, wherein *N*-isopropylacrylamide participates in forming the microcapsule shell, the gradual increase in temperature results in partial degradation of the polymer coagulant dissolved and released in the coagulating acid. Simultaneously, the polymer encapsulated within the microcapsule is gradually released, preventing a rapid decline in the viscosity of the coagulating acid and maintaining a relatively high viscosity retention.

3.1.4. Comparison of Thermal Dilution Properties. The apparent viscosity of the gelling acid system prepared by ordinary gelling agent and gelling agent encapsulated by microcapsules varies with temperature as shown in Figure 6. The experimental results from Figure 6 reveal a gradual decrease in the viscosity of the gelatinous acid system with increasing temperature. The rate of viscosity reduction in the gelatinous acid prepared with GLE-1 is greater than that of GLE-3, indicating that the microcapsule structure can enhance the heat resistance of the gelatinized more effectively. As the temperature rises, intermolecular forces diminish, exerting an

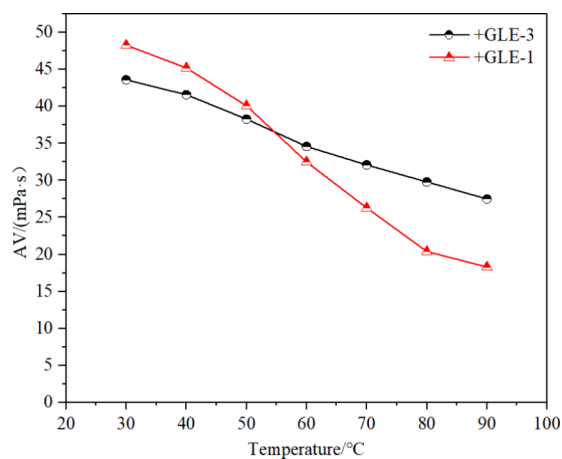


Figure 6. Evaluation results of thermal dilution of GLE-1 and GLE-3 under different temperature conditions.

inhibitory effect on forming the network structure. However, the dissolved polymer continues to be released, maintaining a high viscosity retention. Under the same dosage, the initial viscosity of the gelatinous acid prepared with GLE-1 is higher than that prepared with GLE-3.^{29,30} The polymer material in GLE-3, contributing to viscosity enhancement, is partially encapsulated in microcapsules, resulting in a lower initial viscosity. Nevertheless, with the increase in temperature, the polymer within the microcapsules is gradually released, leading to higher viscosity retention in the gelatinous acid prepared with GLE-3.

3.1.5. Comparison of Antitemperature and Antishear Stability. During the process of injecting gelled acid from the ground into the wellbore, it is subjected to a certain amount of shear action for a certain period of time. Analyzing the effect of shear action on the viscosity of gelled acid has a positive effect on evaluating its effectiveness in the wellbore. The shearing condition was 180 °C, 170 s⁻¹, and the shearing time was up to 60 min. The effect of shear time on the viscosity of gelled acid is shown in Figure 7. From Figure 7, it can be seen that the initial viscosity of the two gelling acids differs by 4.7 mPa·s. Also, as the shear time increases, the viscosity of the gelling acid solution gradually decreases. Meanwhile, the viscosity difference between the gelling acid prepared by GLE-1 and

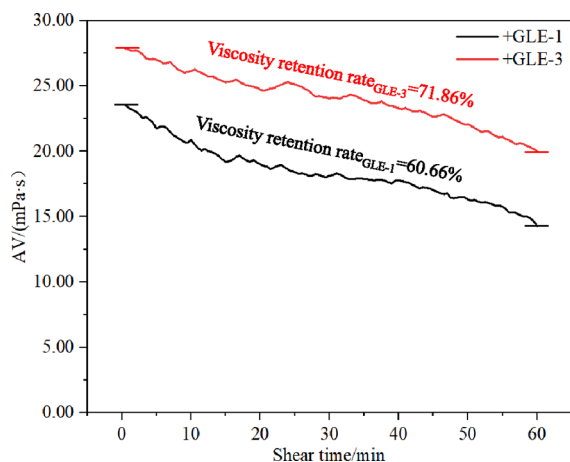


Figure 7. Effect of shear time on the viscosity of gelling acids prepared with GLE-1 and GLE-3.

GLE-3 gradually narrows. After 60 min of shearing, the viscosity of the gelling acid prepared by GLE-3 was higher than that prepared by GLE-1, and the viscosity retention rates of the gelling acid prepared by GLE-1 and GLE-3 after shearing were 79.09 and 88.99%, respectively, indicating better shear stability of the gelling acid prepared by GLE-3. During the shearing process, due to the influence of temperature and solution disturbance, the polymers in the microcapsules is slowly released into the solution, maintaining a good viscosity of the gelling acid prepared by GLE-3.³¹

3.1.6. Slow Performance Evaluation. Figure 8 presents the comparative experimental results of the retarding performance of basic hydrochloric acid, GLE-1, and GLE-3 acid solutions. The results in Figure 8a indicate that at 30 °C, the hydrochloric acid concentration rapidly decreases upon the addition of marble, with a 49% reduction within 1 h and complete reaction after 20 h. In the gelatinous acid systems with the addition of GLE-1 and GLE-3, the rate of acid concentration reduction significantly slows down, suggesting that the gelatinizer effectively retards the reaction rate of acid with the rock. Under the same duration of interaction with marble, the acid concentration in the solution prepared with GLE-1 is higher than that prepared with GLE-3. With equal dosages, the effective content of GLE-1 in the acid solution exceeds that of GLE-3. At 30 °C, the viscosity of the gelatinous acid prepared with GLE-1 is higher than that prepared with GLE-3, leading to a slower reaction rate between the acid solution prepared with GLE-1 and marble compared to that prepared with GLE-3. The curves depicting the change in acid concentration with reaction time for both gelatinous acids reveal that as acid is consumed, the acid concentration in the gelatinous acid system decreases, resulting in a reduced reaction rate with marble. Consequently, with increasing reaction time, the rate of acid concentration decrease diminishes.

The experimental results in Figure 8b demonstrate that at 180 °C, the hydrochloric acid concentration rapidly decreases upon the addition of marble, with a 68.5% reduction after 10 min and complete reaction after 20 min. The retarding performance of the gelatinous acid systems with the addition of GLE-1 and GLE-3 exhibits a pattern completely opposite to that observed under 30 °C conditions. Specifically, under 30 °C conditions, the retarding performance of the gelatinous acid with GLE-1 is superior to that with GLE-3, while at 180 °C, the retarding performance of the gelatinous acid with GLE-1 is inferior to that with GLE-3. At 180 °C, GLE-1 experiences molecular chain elongation and decomposition, and the increased internal energy of molecules at high temperatures leads to insufficient intermolecular forces to constrain the increasingly vigorous molecular movement. This results in larger intermolecular distances, reduced intermolecular attractive forces, decreased internal friction, and, consequently, a decrease in gelatinous acid viscosity. The binding effect on H⁺ weakens, leading to a reduction in its retarding performance.^{32–34} The situation for GLE-3 at high temperatures is similar to that of GLE-1, but due to the microcapsule structure of GLE-3, the high-molecular-weight polymer encapsulated within the capsules can maintain the viscosity of the gelatinous acid through slow release. This feature allows the gelatinous acid prepared with GLE-3 to exhibit excellent retarding performance even at elevated temperatures.

3.2. Antitemperature Mechanism Discussion of GLE-3. GLE-3 has a high viscosity, and the characteristic of the

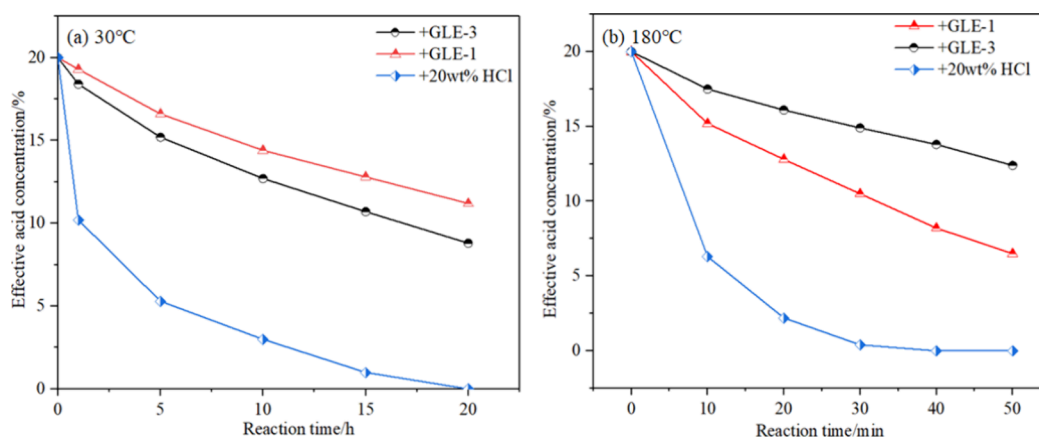


Figure 8. Evaluation results of the slowing performance of different acid solutions under (a) 30 and (b) 180 °C conditions.

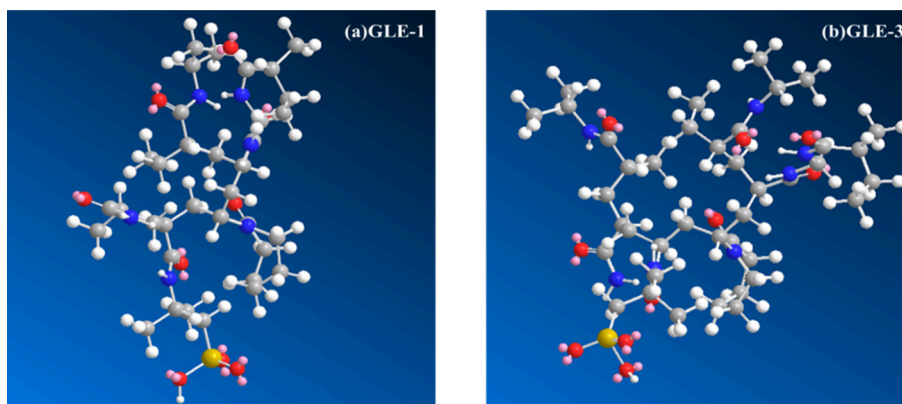


Figure 9. Molecular Configuration Diagram of (a) GLE-1 and (b) GLE-3.

prepared gelling acid is its high viscosity, which can form a network structure, prevent hydrogen ion activity, and delay the reaction between the gelling acid and the reservoir rocks. The mechanism of action of GLE-3 was analyzed through its molecular structure, viscosity of gelling acid, and so forth.

3.2.1. Effect of Thickening. From the molecular structure diagram of GLE-3 (Figure 9), it is evident that GLE-3 is a high-molecular-weight polymer with a carbon–carbon main chain, characterized by a long molecular chain and significant relative molecular mass. Due to the presence of cross-linking agents, GLE-3 assumes a branched structure, allowing intermolecular entanglement to form a network structure within the gelatinous acid system, thereby increasing the viscosity of the gelatinous acid system.³⁵

3.2.2. Delaying the Rate of Acid Rock Reaction. The reaction rate of acid with the formation rock is primarily influenced by two factors: the reaction rate of hydrogen ions in the acid with the solid phase in the formation and the propagation rate of the acid to the reaction interface. The addition of the gelatinized GLE-3 increases the viscosity of the gelatinous acid. According to Fick's law, the network structure formed by the gelatinous acid reduces the migration speed of hydrogen ions in the acid, thereby decreasing the propagation rate of the acid to the rock interface. Simultaneously, the polymers can partially encapsulate the rock, reducing the contact area between hydrogen ions and the formation and decreasing the reaction rate of hydrogen ions with the reactive solid phase.^{8,36} Through these dual mechanisms, the gelatinous acid prepared with GLE-3 can retard the reaction rate of acid

with the rock, allowing H^+ in the acid to penetrate deep into fractures. This facilitates the extension of acid corrosion into deeper layers, ultimately achieving the goal of deep acidification.

3.2.3. Principle of High-Temperature Resistance. Through the analysis of the aforementioned series of experiments, combined with the molecular structural characteristics of microcapsule polymers, the underlying principles governing the controlled release effect of microcapsule gelatinizer under high temperatures are elucidated:^{37–40} (1) for enhancing the rigidity of the molecular main chain: increasing the rigidity of the molecular main chain, such as by increasing the number of carbon atoms polymerized on the main chain or introducing cyclic structures (e.g., benzene rings, polyatomic rings); (2) for introducing strongly polar functional groups in side chains: incorporating strongly polar functional groups in side chains to facilitate hydrogen bonding within and between molecules, thereby enhancing the ability to form a network structure and improving thermal resistance; (3) for increasing molecular complexity through cross-linking: utilizing cross-linking and similar mechanisms to increase the complexity of the molecular chain, thereby reducing molecular thermal motion and enhancing thermal resistance. In the synthesis of GLE-1, the introduction of cross-linking agents results in a more complex molecular structure. The combined effects of cross-linking and hydrogen bonding within and between molecules enhance the polymer's ability to form a complex network structure.^{5,41} The elongated molecular chains contribute to increased rigidity, manifested as an elevation in viscosity. The synergistic action

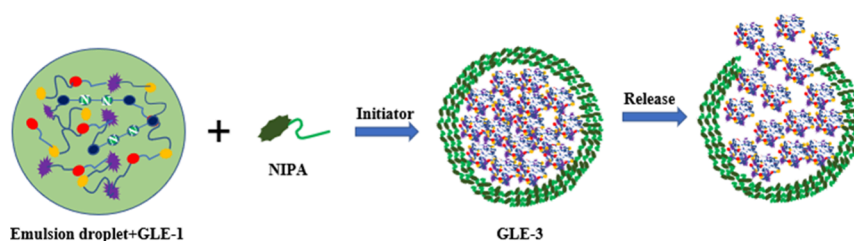


Figure 10. Schematic diagram of GLE-3 microcapsule controlled release principle.

of these three mechanisms enhances the thermal resistance of GLE-1. GLE-3, an advancement of GLE-1, involves the external encapsulation of a poly-*N*-isopropylacrylamide polymer film, creating polymer microcapsules. The encapsulation by the polymer film provides a protective barrier at high temperatures, slowing down the release of internal polymers and reducing their decomposition rate. This enhancement contributes to the improved thermal resistance of the gelling agent (Figure 10).

4. CONCLUSIONS

1. A novel high-temperature-resistant microencapsulated gelatinizer, GLE-3, was synthesized using *N*-isopropylacrylamide as the shell material, acrylamide, 2-acrylamido-2-methylpropanesulfonic acid, and *N*-vinylcaprolactam as the core materials, and *N,N'*-methylenebis(acrylamide) as the cross-linking agent. The preparation involved a reverse emulsion polymerization method, resulting in particles with a predominant size distribution in the range of 10 to 100 μm . GLE-3 exhibited good solubility and dispersion of acid solutions. Furthermore, GLE-3 after polymer microencapsulation has better thermal dilution than GLE-1, making it easier to function under high-temperature reservoir conditions.
2. Under high-temperature conditions, the polymer within the microcapsules of GLE-3 could be slowly released, resulting in superior retarding performance compared to nonmicroencapsulated gelling agents under the same conditions. After a reaction at 180 $^{\circ}\text{C}$ for 50 min, the effective acid concentration retention rate of GLE-3-prepared gelatinous acid increased by 29.5%, highlighting excellent retarding performance.
3. GLE-3 achieved controlled release through a temperature-sensitive effect. At the microscopic level, GLE-3's molecular structure exhibited increased rigidity in the main chain, and the introduction of strongly polar functional groups in side chains enhanced molecular complexity. Under high-temperature cross-linking, the complexity and strength of the acid solution network structure were enhanced, reducing molecular thermal motion and ultimately achieving the high-temperature resistance of microencapsulated gelatinizer. At the macroscopic level, as the temperature increased, the microcapsule walls gradually ruptured, allowing the slow release of the encapsulated high-molecular-weight polymer core material. This prevented the core material of gelling agents from prematurely contributing to high-temperature viscosity maintenance, thereby delaying the reaction rate in acid-rock interactions and achieving deep penetration objectives.

AUTHOR INFORMATION

Corresponding Author

Yunfeng Liu – Research Institute of Natural Gas Technology, PetroChina Southwest Oil & Gasfield Company, Chengdu 610213, China; orcid.org/0000-0002-6851-8792; Email: lyf6280168@126.com

Authors

Lang Zhou – Engineering Technology Department, PetroChina Southwest Oil & Gasfield Company, Chengdu 610056, China

Xiaochun Wan – Development Department, PetroChina Southwest Oil & Gasfield Company, Chengdu 610056, China

Yongfan Tang – Research Institute of Natural Gas Technology, PetroChina Southwest Oil & Gasfield Company, Chengdu 610213, China

Qiang Liu – Engineering Technology Department, PetroChina Southwest Oil & Gasfield Company, Chengdu 610056, China

Wei Li – Research Institute of Natural Gas Technology, PetroChina Southwest Oil & Gasfield Company, Chengdu 610213, China

Jianbo Liao – Northwest Branch, Research Institute of PetroChina Exploration & Development, Lanzhou 730020, China

Complete contact information is available at: <https://pubs.acs.org/10.1021/acsomega.3c09586>

Author Contributions

All authors have accepted responsibility for the entire content of this manuscript and approved its submission.

Notes

The authors declare no competing financial interest.

ACKNOWLEDGMENTS

This research was financially supported by the CNPC Major Technology Project (no. 2023ZZ16), the Postdoctoral Project of PetroChina Southwest Oil & Gasfield Company (no. 20220302-19), the Innovation Consortium Project of PetroChina Southwest Oil & Gasfield Company (no. 2020CX0105), and the China Petroleum Exploration and Production Company Technology Project (no. 2022KT1703).

REFERENCES

- (1) Mohsen, F.; Abbas, T.; Stefan, L.; Alireza, K. The influence of acidizing on propped fractures for productivity enhancement: Eagle Ford laboratory study [J]. *Fuel* **2022**, No. 125363, DOI: 10.1016/j.fuel.2022.125363.
- (2) Yue, H.; Liu, F.; Zhang, H.; Zhou, C.; Chen, W.; Xiao, Z. Specified staged acid fracturing of horizontal well for strong-heterogeneity carbonate gas reservoirs: A case study on the gas

reservoir of the fourth member of Upper Sinian Dengying Formation in Gaoshiti-Moxi area of the central Sichuan Basin [J]. *Natural Gas Industry B* **2021**, *8* (5), 484–493.

(3) Wu, Y.; Jiang, Q.; Du, J. Preparation and Performance Evaluation of Dual Slow Acid in High Temperature Carbonate Reservoir [J]. *Oilfield Chem.* **2023**, *40* (03), 386–393.

(4) Abdollahi, R.; Esfandiyari, H.; Nadri Pari, M.; Davarpanah, A.; et al. Conventional diverting techniques and novel fibr-assisted self-diverting system in carbonate reservoir acidizing with successful case studies [J]. *Pet. Res.* **2021**, *6* (3), 247–256.

(5) Zhou, L.; Guo, A.; Wang, X.; Qiao, J.; Tang, X.; et al. The effect of temperature, natural fractures and vugs on the acidizing process in fractured-vuggy reservoirs with hydro-thermal-chemical coupled modeling [J]. *J. Pet. Sci. Eng.* **2022**, *213*, No. 110416.

(6) Xu, H.; Cheng, J.; Zhao, Z.; Lin, T.; Liu, G.; Chen, S. Coupled thermo-hydro-mechanical-chemical modeling on acid fracturing in carbonate geothermal reservoirs containing a heterogeneous fracture [J]. *Renewable Energy* **2021**, *172*, 145–157.

(7) Wang, C. X.; Gao, J. L.; Zhang, X. B. Effect of Mixed Acid Fluid on the Pore Structure of High Rank Coal and Acid Fluid Optimization [J]. *ACS Omega* **2022**, *7* (37), 33280–33294.

(8) Wang, J. Y.; Jia, J. H.; Zhao, X. T.; et al. Study of a High Temperature Acidizing Gelatinizer YJN-1 [J]. *Oilfield Chem.* **2007**, *24* (2), 113–116.

(9) Li, H.; Luo, B.; Li, Q.; et al. Preparation and Performance Evaluation of Acid Gelling Agent with High Temperature Resistance [J]. *Oilfield Chemistry* **2022**, *39* (04), 589–594.

(10) Sui, Y.; Cao, G.; Guo, T.; Li, Z.; Bai, Y.; Li, D.; Zhang, Z.; et al. Development of gelled acid system in high-temperature carbonate reservoirs [J]. *J. Pet. Sci. Eng.* **2022**, *206*, No. 110836.

(11) Wang, M.; Che, G. M.; Zhou, C. L.; et al. A Novel Gelled Acid for the Acid Fracturing of the High-Temperature Carbonates and its Application [J]. *Drill. Fluid Completion Fluid* **2020**, *37* (5), 670–676.

(12) Sun, Y. D.; Yang, L.; Li, X. L. Development and Performance Evaluation of Hybrid Gelling Agent for Acidification at High Temperature [J]. *Oilfield Chem.* **2023**, *40* (2), 223–228.

(13) Al-Shargabi, M.; Davoodi, S.; Wood, D. A.; Ali, M.; Rukavishnikov, V. S.; Minaev, K. M.; et al. A critical review of self-diverting acid treatments applied to carbonate oil and gas reservoirs [J]. *Pet. Sci.* **2023**, *20* (2), 922–950.

(14) Liu, Y. F.; Zhou, L.; Tang, Y. F.; et al. Synthesis and Characterization of a Resin/Acrylamide-2-acrylamide-2-methylpropane Sulfonate-Diallyl Dimethyl Ammonium Chloride-N-vinyl-2-pyrrolidinone Polymer Microcapsule Gelling Agent for Oil and Gas Field Transformation [J]. *ACS Omega* **2023**, *8* (51), 49080–49087.

(15) Liu, Y. F.; Tang, Y. F.; Chang, Q. H.; et al. Development of a novel heat- and shear-resistant nano-silica gelling agent [J]. *Nano-technol. Rev.* **2022**, *11* (1), 2786–2799.

(16) Jiang, D. S.; Li, X. P.; Jiang, K. W.; et al. Study on diverting acid conductivity of heterogeneous reservoir in Gaomo area [J]. *Chem. Eng. Oil Gas* **2021**, *50* (4), 92–95.

(17) Li, L. N. *Experimental study on microencapsulation process of high water absorbent resin [D]*; China University of Geosciences, Beijing, 2008: 27–42.

(18) Song, L.; Chen, Y. L.; Huang, R. Study on the preparation and efficacy evaluation of azelaic acid microcapsule [J]. *Deterg. Cosmet.* **2019**, *42* (01), 27–30.

(19) Singh, R.; Panthi, K.; Mohanty, K. Microencapsulation of Acids by Nanoparticles for Acid Treatment of Shales [J]. *Energy Fuels* **2017**, *31* (11), 11755–11764.

(20) Zhang, R. S.; Wang, Z. B.; Zhao, M. Y.; et al. Preparation and Performance Evaluation of Helper-breaking Capsule Type Shielding Temporary Plugging Protection Agent in Fracturing [J]. *Oilfield Chem.* **2019**, *36* (02), 225–229.

(21) Ji, Y. F.; Yang, Y.; Cao, X. L.; et al. Development and evaluation of microencapsulated emulsion polymer flooding agent [J]. *Acta Pet. Sin.* **2023**, *44* (6), 975–982.

(22) Essifi, K.; Brahmi, M.; Berraouan, D.; Amrani, A.; El Bachiri, A.; Laure Fauconnier, M.; Tahani, A.; et al. Development and

characterization of alginate@montmorillonite hybrid microcapsules for encapsulation and controlled release of quercetin: Effect of clay type [J]. *Mater. Today: Proc.* **2023**, *72* (7), 3280–3286.

(23) Kanti Chattopadhyay, P.; Ranjan Singha, N. MOF and derived materials as aerogels: Structure, property, and performance relations [J]. *Coord. Chem. Rev.* **2021**, *446*, No. 214125.

(24) Wang, X.; Jia, W. F.; Ren, Q. Q.; et al. Development and Evaluation of a New Emulsified Gelled Acid [J]. *Drill. Fluid Completion Fluid* **2017**, *34* (5), 111–116.

(25) Du, J.; Guo, G. X.; Liu, P. L.; et al. Experimental Study on the Autogenic Acid Fluid System of a High-Temperature Carbonate Reservoir by Acid Fracturing [J]. *ACS Omega* **2022**, *7* (14), 12066–12075.

(26) Zhang, Y. D.; Wu, W. G.; Jing, X. W.; et al. Performance evaluation and field application of variable viscosity fracturing fluid system for tight gas reservoir [J]. *Chem. Eng. Oil Gas* **2022**, *51* (1), 73–77.

(27) Monette, M.; Nguyen, Q. An Experimental Study of Wormhole Morphology with a Novel Acid System in Ultra-High-Temperature Carbonate Reservoirs [J]. *Transport Porous Media* **2023**, *149*, 625–642.

(28) Wang, Y. J.; Zhou, F. J.; Su, H.; et al. Performance evaluation of microemulsion acid for integrated acid fracturing in Middle Eastern carbonate reservoirs. *Petroleum Exploration and Development* **2023**, *50* (5), 1196–1205.

(29) Al-Nakhli, A.; Ibrahim, Z.; Ahmed, D.; et al. A Novel Approach to Improve Acid Diversion Utilizing In-Situ Foam Generating Fluids [C]. *Abu Dhabi International Petroleum Exhibition and Conference*; SPE: SPE-203330-MS, 2020.

(30) Aliu, A. O.; Guo, J.; Wang, S.; Zhao, X.; et al. Hydraulic fracture fluid for gas reservoirs in petroleum engineering applications using sodium carboxy methyl cellulose as gelling agent [J]. *J. Nat. Gas Sci. Eng.* **2016**, *32*, 491–500.

(31) Kavitha, T.; Kang, I. K.; Park, S. Y. Poly(N-vinyl caprolactam) grown on nanographene oxide as an effective nanocargo for drug delivery [J]. *Colloids Surf., B* **2014**, *115*, 37–45.

(32) Ibrahim, A. A.; Prasad, K.; Yahya, H. A.; et al. The Future of Fracture Acidizing: A Low pH, Robust, and Residue-Free Crosslinked Fracturing Fluid [C]. *Abu Dhabi International Petroleum Exhibition and Conference*; SPE SP-182891-MS, 2016.

(33) Shi, Y.; Xu, K.; Weng, D. W.; et al. Temperature resistance mechanism of modified partially hydrolyzed polyacrylamide based on molecular dynamics simulation [J]. *Chem. Eng. Oil Gas* **2023**, *52* (3), 76–80.

(34) Yuan, L.; Wang, Y.; Li, Q.; et al. Evaluation of a control-released in-situ generated acid tablet for acid fracturing [J]. *J. Pet. Sci. Eng.* **2019**, *174*, 384–393.

(35) Liao, Y.; Zhang, D.; Peng, J.; Liang, H.; Gong, Y.; et al. Measurement of Reaction Rate of Gelled Acids and Calcite with the Rotating Disk Apparatus [J]. *Nat. Res.* **2017**, *8*, 559–568.

(36) Zhang, L.; Zhou, F.; Mou, J.; et al. A new method to improve long-term fracture conductivity in acid fracturing under high closure stress [J]. *J. Pet. Sci. Eng.* **2018**, *171*, 760–770.

(37) Deb Roy, J. S.; Deb, M.; Sanfui, M. H.; Roy, S.; Dutta, A.; Chattopadhyay, P. K.; Ghosh, N. N.; Roy, S.; Singha, N. R.; et al. Light-Emitting Redox Polymers for Sensing and Removal-Reduction of Cu(II): Roles of Hydrogen Bonding in Nonconventional Fluorescence [J]. *ACS Appl. Polym. Mater.* **2022**, *4* (3), 1643–1656.

(38) Mitra, M.; Sanfui, M. H.; Roy, S.; Deb, M.; Roy, C.; Dutta, A.; Ghosh, N. N.; Rahaman, M.; Chattopadhyay, P. K.; Roy, S.; Singha, N. R.; et al. Synthesis of Intrinsically Dual-Emissive Aliphatic Conducting Polymer and ESIPT-Associated Switching of Amide-Aggregate to Imidol-Aggregate for Sensing of Cr(III) and Fe(III) [J]. *Macromolecules* **2023**, *56* (22), 9078–9096.

(39) Zhao, W.; Xiong, Y.; Dai, Y. M.; et al. Synthesis and performance study of a hydrophobic association polymer PAAD-18 for volume fracturing [J]. *Chem. Eng. Oil Gas* **2023**, *52* (2), 70–75.

(40) Wenfeng, J.; Chenggang, X.; Bao, J.; Junwen, W. A high temperature retarded acid based on self-assemblies of hydrophobically

associating polymer and surfactant [J]. *J. Mol. Liq.* **2023**, *370*, No. 121017.

(41) Zhang, N. L.; Chen, X.; Luo, Z. F.; et al. Experimental study of fracture conductivity in dolomite reservoirs treated with different acid fracturing technologies. *Geoenery Science and Engineering* **2023**, *227*, No. 211914.